

STRAIN EVALUATION OF PEEK CANTILEVER BARS AROUND IMPLANTS ASSISTED MANDIBULAR OVERDENTURES (IN VITRO STUDY)

Rania M. Abd El Moaty^{1*} BDS, Magdi A. Awadallah² PhD,
Mona S Mostafa³ PhD

ABSTRACT

INTRODUCTION: A unilateral partial denture is a treatment option for unmodified Kennedy class II cases. But from a biomechanical point of view regarding stability and stress distribution possibly insufficient. The incorporation of the glass abutment in the unilateral partial denture may add to the design; by improving the stress distribution hence, decrease the exaggerated loads conducted to the supporting structures.

OBJECTIVES: This study aimed at measuring and comparing the strain on the supporting structures of class II tooth-tissue supported telescopic partial denture with different prosthetic designs.

MATERIALS AND METHODS: Three groups of class II maxillary telescopic partial dentures were constructed of BioHPP using CAD/CAM. Each group contained six specimens; Group A class II partial denture with cross arch stabilization and without using the glass abutment, Group B class II partial denture with cross arch stabilization supported distally with the glass abutment at the second molar tooth and Group C class II partial denture without cross arch stabilization supported distally with the glass abutment at the second molar tooth. Using a universal testing machine and strain gauge, stress around the abutment teeth and the distal extension saddle was measured on an epoxy model missing first and second molars under 200N vertical and oblique loads.

RESULTS: There was a statistically significant difference in the microstrains developed at all the examined sites between the three groups (ANOVA test $p < 0.001$). During vertical and oblique loading, the highest mean microstrains were recorded distal to the second premolar, in all groups. The use of glass abutment in groups B and C had reduced the microstrains conducted to the distal aspect of the abutments significantly than in group A.

CONCLUSIONS: Reduction of stress to the abutment teeth was observed when using the glass abutment, which has allowed redistribution of load between the abutments and the ridge.

KEYWORDS: Unilateral distal extension removable partial dentures, Kennedy Class I, glass abutment, Stress analysis, Strain gauge, Telescopic attachment, CAD/ CAM partial dentures, BioHPP.

1 Bachelor of Dentistry, Faculty of Dentistry, Alexandria University, Alexandria, Egypt.

2 Professor of Prosthodontics, Removable Prosthodontics Department, Faculty of Dentistry, University of Alexandria, Alexandria, Egypt.

3 Lecturer of Prosthodontics, Removable Prosthodontics Department, Faculty of Dentistry, University of Alexandria, Alexandria, Egypt.

*Corresponding author:

E-mail: rania.mokhtar@yahoo.com

INTRODUCTION

Posterior free end edentulous areas are the most common partially edentulous clinical situations. Prosthetic treatment with removable overdentures can be challenging when a fixed bridge cannot be inserted due to the absence of a distal post. Rehabilitation with removable partial overdentures (RPODs) is a conservative and low-cost solution for the prosthetic management of patients with shortened dental arches suffering from a functional or an aesthetic problem for the replacement of posterior teeth (Kennedy Class I and II) (1,2).

The absence of posterior posts (implant or tooth) to retain and support RPDs compromises the prognosis of the prosthetic treatment. Insufficient support, retention, and stability is usually accompanying the distal extension removable partial dentures (DERPDs). The restoration of DERPDS requires planning according to biomechanical design principles. Obtaining adequate support, retention, and stability from both the ridge and supporting posts should be designed without provoking any harm to the supporting structures (2).

Restoring unmodified class II Kennedy cases with DERPDS is even more challenging due to the patient dissatisfaction when comparing it with the intact side or showing objection and intolerance to the bulky design, which has to cross the arch to the intact side (3).

Various design concepts were suggested to solve this issue, among which the use of a unilateral design restoration (a unilateral partial denture); that does not cross the arch to the other side was considered as a better option for these cases using either clasps or attachments (3-6).

Telescopic attachment provides adequate direct retention, proper stress distribution, and indirect retention while still satisfying the esthetic requirements by eliminating conventional metal clasps. They transfer forces throughout the direction of the long axis of the abutment teeth providing guidance, support, and protection from movements that may displace the RPD (7).

Moreover, the recent material generations provide exceptional biomechanical characteristics to manage stresses that became near to the physiologic limit of the supporting structures. A modified Polyether ether ketone (PEEK) material containing 20% ceramic fillers is a Bio High-Performance Polymer (BioHPP) that confers high biocompatibility, good mechanical properties, high-temperature resistance, and chemical stability. High-performance polymers have great potential as framework material, both for fixed and removable dental prostheses. The Elastic modulus of BioHPP lies in the range of 4000 MPa, which very strongly resembles the elasticity of human bone. BioHPP frameworks, therefore, act as cushion during chewing and have a high resistance to abrasion and decay, it also has low density, this makes the prosthesis very light in weight which improves patient comfort (8).

The ZX-27 glass abutment was launched to be used in the fixed partial denture to support the cantilevered pontic or pontics in long-span fixed bridges (9).

It is made of exceptional material (borosilicate glass) and adheres to the underlying mucosa in the edentulous segments of the dental arches. The borosilicate glass is 100% biocompatible because it does not contain lead as normal glass (10).

The glass abutment is very flexible at the melting temperature (1560-1600 C). It can take the shape of any structure at that temperature with the most accurate details. On cooling, it has a high modulus of elasticity (69.000 MPa) (9).

The distribution scheme of the mastication forces is unique; the force takes an arch-shape spread. The system uses the concept of vacuum and adhesion to fix the bridge on the underlying mucosa (11).

Accuracy and adaptation play an essential role in preventing undue forces on the abutments. Accurately adapted and properly manufactured RPDs using CAD/CAM technology will decrease damaging stresses on the abutments and maintain their health. Multiple steps in the traditional fabrication techniques lead to improperly adapted and inaccurate RPD (1,2,12).

A variety of techniques was used in biomechanical investigations for both in-vitro and in-vivo studies, and yet no sole technique met all of the requirements for illustration of the ample physiological interactions involved. Complex analytical methods such as photogrammetry and finite element analyses are now possible because of the convenience of high-capacity computer systems. However, strain gauge measurements were the implemented methodology in this study as they are the most accurate and widely used instruments to record surface stresses and to study the mechanics of prosthetic appliances in former researches (13).

MATERIALS AND METHODS

This in-vitro study was conducted on a commercially available educational acrylic maxillary model with acrylic teeth which can be inserted and removed from the model (Nissin dental products ineKyoto Japan).

Model construction

The first and second molars were withdrawn from the acrylic model on one side and their root sockets were blocked with molten base plate wax (Cavex Set up Regular modeling Wax, Holland BV, Haarlem, the Netherlands). An impression for this altered cast was made using silicone rubber base impression (Impregum Soft, 3M™ ESPE™, St. Paul, USA).

The roots of abutment teeth were wrapped with 0.2- 0.3 mm thickness tin foil and reinserted in their conforming positions in the impression. Epoxy resin (Specifix, Stuers, Willich, Germany) was poured into the impression and was left to harden. The acrylic teeth with the spacer were then removed from the epoxy resin model. Rubber base adhesive (3M™ ESPE™ VPS Tray Adhesive, 3M™ ESPE™, St. Paul, USA) was painted on the sockets and the root portions of the abutment teeth and allowed to dry for 10 minutes. Light body Poly Vinyl Siloxane (PVS) impression material (Express™ 2 Light Body Flow, 3M™ ESPE™, St. Paul, USA) was administered in the sockets of the abutment teeth before repositioning of these teeth in their sockets. This was done to simulate the periodontal ligament (PDL). A stone index (Type IV dental stone material, Syna-Rock, DFS-DIAMON, Germany), was made over the epoxy resin model and extended on the model buccally and palatally to act as a stopper for precise repositioning. 4mm thickness was reduced from the surface of the model. The reduced areas

were then painted with rubber base adhesive, and allowed to dry for 10 minutes. The fitting surface of the stone was packed with light body PVS and then repositioned over the reduced area with firm hold until complete polymerization. The epoxy resin model was removed from the stone index after setting of the PVS (14,15). For the casts that were used for the unilateral design oral mucosa simulation was only carried out for the residual ridge, there was no need to cover the palate.

Telescopic abutment teeth (the first and second premolars on the edentulous side) were prepared following the principles described by Körber (16), with a common path of insertion to receive telescopic crowns. Each abutment was prepared using a tapered round end stone to 5mm length, deep chamfer finish line with a width of 1.5 mm at the gingival level. Walls were prepared with a taper of 10-12° and uniform anatomical axial and occlusal reduction of 2.5 mm. Parallelism of the abutments to each other and the long axis was insured using a dental surveyor (Ney surveyor, Dentsply Sirona, USA). Rest seat preparation for the double Akers' clasp was carried out on the distal of the second premolar and mesial of the first molar, and a rest seat for the indirect retainer on the mesial of the first premolar of the intact side, in the casts that were used to fabricate the dentures with cross arch stabilization.

Construction of primary copings (CAD/CAM)

The digitalization of the abutment teeth was performed by scanning the epoxy model with the prepared teeth via a 3D desktop optical scanner (S600 ARTI Scanner from Zirkozahn, USA). 3Shape Dental System™ (3Shape A/S, Denmark) software was used to design the primary copings with a 2° taper and a deep chamfer finish line. The thickness of the framework was set at 0.7mm. An order was given to the milling machine (CNC milling machine, VHF SI AG, Germany) to mill it in BioHPP (Bredent GmbH, Senden, Germany). The prepared acrylic abutment teeth and the fitting surface of the primary copings after air abrasion were conditioned using a special adhesive bonding of composite to plastics Visio.link (Bredent GmbH, Senden, Germany) and light-cured following the manufacturer's instructions, and then, the primary copings were permanently cemented to the prepared abutments (Figure 1a,2a,3a) using a Dual-cured adhesive composite Combo.lign (Bredent GmbH, Senden, Germany).

Adaptation of the glass abutment

A stone duplicate of the study model was made to be used for the adaptation of the glass abutment. The glass abutment was mounted on the abutment holder and was heated to the required melting temperature of around 1600° C according to the manufacturer (9,11). The melted glass was pressed

on the stone cast at the site of the second molar tooth. When it cooled, it was shortened and prepared like the natural abutment teeth.

Construction of secondary copings and frameworks (CAD/CAM)

The epoxy models with the primary copings cemented to the abutment teeth were duplicated in stone to enable outlining the design and inscribing the bead lines. The design was outlined and bead lines were inscribed on the stone duplicates of the study models after cementation of the primary copings. The glass abutments were then fixed to the stone models at the site of the second molar tooth using cervical wax (Cera Reus, SA, Reus, Spain). The same machines and materials used in the fabrication of primary copings were used to scan, survey, design, and mill the denture frameworks with the secondary telescopic crowns and the pontic teeth. After cautious finishing and polishing of the RPD, it was tried on the stone models for complete seating. The glass abutments were then cleaned, conditioned with K-Primer (Silicate ceramics and glass-ceramics primer) (Bredent GmbH, Senden, Germany), and cemented to their corresponding primed copings using Combo.lign adhesive.

Veneering of BioHPP

Veneering of the teeth

Veneering of secondary telescopic crowns and pontic teeth was carried out using breCAM.HIPC blanks (Bredent GmbH, Senden, Germany). Teeth were scanned using the same machines and techniques used for fabrication of primary copings and RPDs, veneers were designed with 1mm thickness and a spacer of 120µ between the framework and veneers according to the recommended values of the manufacturer. Teeth frameworks and veneers were air abraded and conditioned using the same composite resin primer visio.link. Veneers were cemented to frameworks using a dentin-colored dual-polymerizing adhesive composite resin (Combo.lign) of the same shade.

Veneering of the buccal flange

A pink shade indirect light-polymerized nanofilled composite resin facing material (Crea.lign) (Bredent GmbH, Senden, Germany) was layered free hand to imitate soft tissues. After polymerization, the veneering composite was finished and polished. The telescopic RPDs were then seated on the epoxy models (Figure 1b,2b,3b).

Installation of Strain Gauges

The strain gauges used in this study were supplied with a fully encapsulated grid and connected wires. The strain gauges (Kyowa electronic instrument co., Tokyo, Japan) used in this study had a self-protected linear gauge, 1 mm length and 2.4mm width, with gauge resistance 119.6 ± 0.4 , gauge factor $2.13\% \pm 1.0\%$, adoptable thermal expansion $11.7 \text{ ppm}/^\circ\text{C}$ and temperature coefficient

of gauge factor $+0.08\%/^{\circ}\text{C}$. Eight sites were selected on each model for the installation of strain gauges; mesial to the first premolar abutment, distal to the second premolar abutment, buccal and palatal to each premolar abutment, and on the ridge at the first and second molars sites. Preparation of the proposed sites was made using diamond stones by thinning the acrylic resin buccally, palatally, distally, and mesially around the abutment teeth to a thickness of about 1 mm; ending short of the base of the model and parallel to the long axis of the roots of the abutment teeth. The epoxy resin of the model around the two premolar abutment teeth was reduced into a cuboid-shaped area, leaving approximately 1mm thickness of epoxy resin covering the roots of the abutment teeth starting from the crest of the ridge till the root apices. The surfaces were prepared to be flat and parallel to the long axis of the roots of the abutment teeth in all directions. For the crest of the ridge, the preparations were done at the site of the central fossa of the first and second molar teeth. At the end of the preparation, small holes were drilled in the acrylic resin from the crest to the bottom of the base corresponding to each strain gauge to allow the wires to pass through it. The prepared acrylic surfaces were then smoothed with fine grit aluminum oxide sandpaper to develop a surface texture suitable for strain gauge bonding. The strain gauges were adhered using alpha cyanoacrylate adhesive (CC-33AEP-34B Strain Gauge cement, Kyowa Electronic Instruments CO Japan). The wires of the gauges were labeled and fastened to the model base by adhesive tapes to avoid any possible movement of the wires that may affect the precision of the readings (Figure4). The strain gauges were labeled with a code to identify them during measurements as Follows; M4 (mesial four), B4 (buccal four), P4 (palatal four), D5 (distal five), B5 (buccal five), P5 (palatal five), R6 (ridge at the site of six) and R7 (ridge at the site of seven).

The loading device universal testing machine (Mecmesin, multitest5- xt, USA), was used in compression mode to apply vertical and oblique loads. The machine was programmed to apply a static load started from zero up to 200 N at an increasing constant rate (crosshead speed) of 10 mm/min. A strainmeter (Data Logger model TDS-150 Manufactured by TML, Tokoyo, Japan) was used to record the microstrains conducted to each strain gauge. The strainmeter was then connected to a personal computer with the aiding of special software to allow for measuring the microstrains that resulted from the applied load. All the connected gauges were tested before the load application to ensure that they are working. Load applicator rod of the testing machine was applied to the denture at the central fossa of the first molar tooth. The vertical load was applied (Figure5) then the oblique load (Figure6). The applied static load

started from zero up to 200 N. The microstrains of the eight strain gauges were recorded to measure the strains developed at the determined sites. Enough time was passed (about 15 minutes) between every two successive measures to permit complete recoil of the resilient structure.

Statistical analysis

Data were introduced to the computer and analyzed using IBM SPSS software package version 20.0. (Armonk, NY: IBM Corp). The Kolmogorov-Smirnov test was used to verify the normality of distribution of the quantitative data; which was found to be normally distributed. Repeated measures ANOVA was used to compare and test possible differences between the three designs, and the Post Hoc test (Tukey) for pairwise comparisons was used to determine significant differences between the mean microstrains ($\mu\text{m}/\text{m}$) when ANOVA test was significant. The significance of the obtained results was judged at the 5% level.

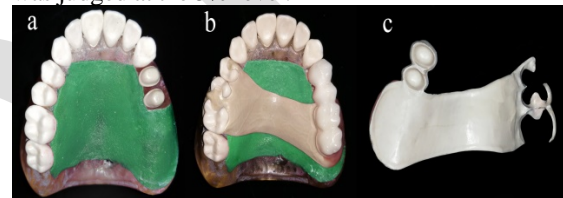


Figure 1: (a) group A epoxy model with the primary copings permanently cemented to the prepared abutments, (b) group A telescopic RPD with the conventional bilateral design seated on the epoxy model, (c) The tissue surface of the RPD.

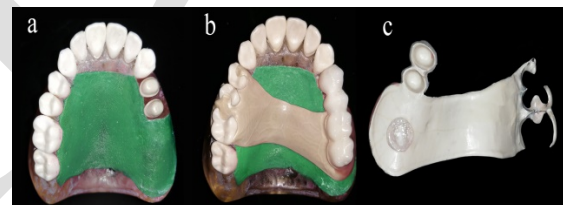


Figure 2: (a) group B epoxy model with the primary copings permanently cemented to the prepared abutments, (b) group B telescopic RPD with the bilateral design using the glass abutment seated on the epoxy model, (c) The tissue surface of the RPD showing the glass abutment.

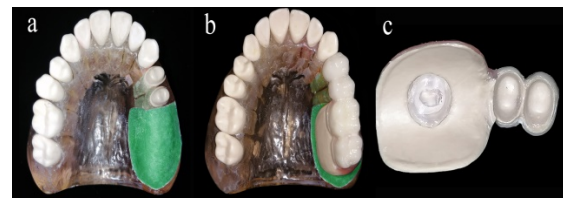


Figure 3: (a) group C epoxy model with the primary copings permanently cemented to the prepared abutments, (b) group C telescopic RPD with the unilateral design using the glass abutment seated on the epoxy model, (c) The tissue surface of the RPD showing the glass abutment.

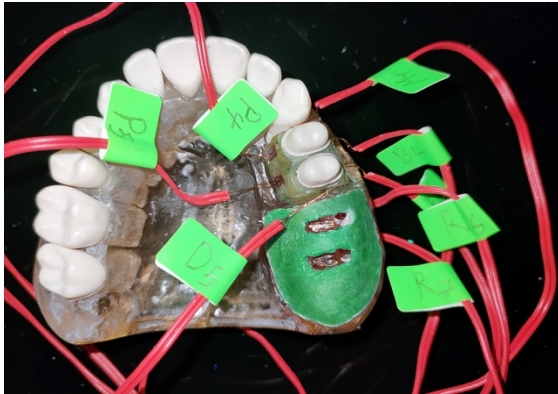


Figure 4: Labeled strain gauges installed to its prepared sites on the model.

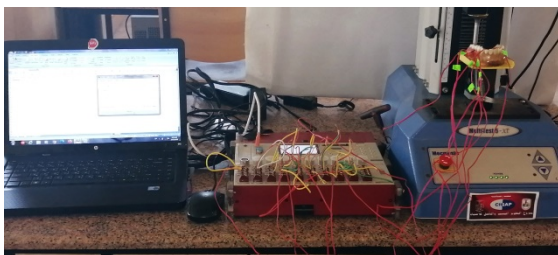


Figure 5: Vertical loading test.

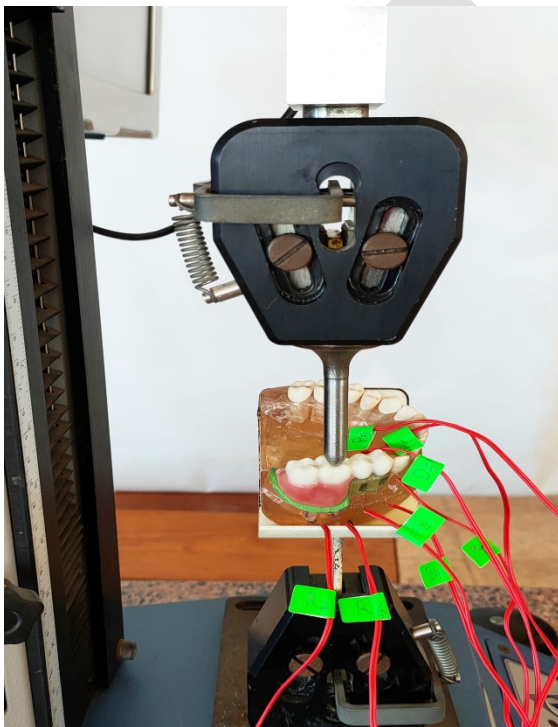


Figure 6: Oblique loading test.

RESULTS

This study aimed at evaluating and comparing the mean microstrains around the abutment teeth and the distal extension saddle in three designs of RPDs under vertical and oblique loads using a strain gauge.

Means and standard deviations (SD) of microstrains ($\mu\text{m/m}$) around abutment teeth and

supporting ridge for different designs and loading conditions are presented in (Table 1 and 2), where the negative sign denotes compression while, absence of sign denotes tension following load application.

The mean values of microstrains developed after load application at all the tested aspects of the abutment teeth were summed and compared to determine the total microstrains affecting the abutment teeth.

There was a statistically significant difference in the mean microstrains developed at all the examined sites between the three groups (ANOVA test $p < 0.001$) during both vertical and oblique loading.

During vertical loading

Microstrains conducted to the abutment teeth

There was a statistically significant difference in the value of the sum of microstrains developed around the abutment teeth (ANOVA test $p < 0.001$), Post Hoc Test (Tukey) for pairwise comparison between each two groups revealed that group A demonstrated a significantly higher mean microstrains around the abutment teeth than the two other groups ($2856.6 \pm 82.92 \mu\text{m/m}$), followed by group C ($2054.0 \pm 33.48 \mu\text{m/m}$) while group B recorded the lowest mean microstrains ($2011.6 \pm 28.57 \mu\text{m/m}$). But, despite having a higher mean microstrain, the difference between group C and B was insignificant.

For all the test groups the highest microstrain was recorded distal to the second premolar abutment compared to other aspects of abutment teeth, being significantly higher in group A ($1513.9 \pm 62.15 \mu\text{m/m}$) than the two other groups, group C recorded higher mean microstrains ($938.8 \pm 16.44 \mu\text{m/m}$) than group B, but the difference was insignificant.

Microstrains conducted to the ridge

On the contrary to the microstrains conducted to abutment teeth, the mean microstrains conducted to the ridge at the site of the second molar were significantly lower in group A ($26.47 \pm 2.14 \mu\text{m/m}$) than the two other groups, while group C recorded higher mean microstrains ($157.0 \pm 6.87 \mu\text{m/m}$) than group B ($153.5 \pm 6.37 \mu\text{m/m}$), but the difference was insignificant.

While at the first molar site (site of load application), group A recorded a significantly higher mean microstrain ($45.17 \pm 3.46 \mu\text{m/m}$) than the other groups, group C recorded higher mean microstrains ($29.88 \pm 3.95 \mu\text{m/m}$) than group B ($27.50 \pm 3.17 \mu\text{m/m}$), but the difference was insignificant.

During oblique loading

Microstrains conducted to the abutment teeth

There was a statistically significant difference in the value of the sum of microstrains developed around the abutment teeth (ANOVA test $p < 0.001$), Post Hoc Test (Tukey) for Pairwise comparison

between each two groups revealed that group C demonstrated the highest mean microstrains around the abutment teeth ($2968.6 \pm 35.07\mu\text{m/m}$), followed by group A ($2898.8 \pm 85.76\mu\text{m/m}$), with no statistically significant difference.

Group B recorded the lowest mean microstrains ($2317.7 \pm 80.96\mu\text{m/m}$), that was significantly lower than group A. But the difference between group B and group C was statistically insignificant.

For all the test groups, the highest mean microstrains were recorded distal to the second premolar abutment compared to other aspects of abutment teeth. Group A recorded the highest mean microstrain ($1254.2 \pm 40.01\mu\text{m/m}$), followed by group C ($1224.4 \pm 25.14\mu\text{m/m}$), with no statistically significant difference. While group B recorded the lowest mean microstrain ($1093.3 \pm 80.60\mu\text{m/m}$) that was significantly lower than the two other groups.

Microstrains conducted to the ridge

The highest mean microstrains conducted to the ridge was recorded at the site of the second molar (site of glass abutment) in group B ($111.8 \pm 8.29\mu\text{m/m}$) that was significantly higher than the other groups. Group A ($22.60 \pm 2.06\mu\text{m/m}$) was also significantly lower than group C ($96.64 \pm 6.72\mu\text{m/m}$).

While at the first molar site (site of load application), group A recorded the highest mean microstrains ($35.29 \pm 2.14\mu\text{m/m}$), which was significantly higher than the other groups, followed by group C ($28.67 \pm 3.72\mu\text{m/m}$) that was also significantly higher than group B ($20.79 \pm 2.31\mu\text{m/m}$).

Table 1: Comparison between the recorded microstrain values ($\mu\text{m/m}$) for group A, B and C recorded at the examined sites under vertical load represented with range, mean and standard deviation.

Site of gauge	Group A (n = 6)	Group B (n = 6)	Group C (n = 6)	F	p
M4					
Mean \pm SD.	-41.8 \pm 4.7	-65.3 ^a \pm 2.3	-67.2 ^a \pm 1.7	117.74*	<0.001*
Median (Min. – Max.)	41.9 (34.7 – 47.8)	64.8 (62.4 – 68.8)	67.1 (65.3 – 69.9)		
B4					
Mean \pm SD.	-60.6 \pm 6.9	-86.1 ^a \pm 8.1	-89.4 ^a \pm 5.5	31.215*	<0.001*
Median (Min. – Max.)	60.6 (50.2 – 69.4)	85.1 (74.5 – 99.4)	87.8 (84.8 – 99.9)		
P4					
Mean \pm SD.	-136.3 \pm 8.3	-108.2 ^a \pm 8	-115.2 ^a \pm 6.8	21.545*	<0.001*
Median (Min. – Max.)	138.6 (120.7 – 144.7)	104.9 (99.9 – 118.7)	116.5 (105.8 – 122.7)		
D5					
Mean \pm SD.	-1513.9 \pm 62.2	-925.3 ^a \pm 27.6	-938.8 ^a \pm 16.4	414.99*	<0.001*
Median (Min. – Max.)	1524.3 (1427.8 – 1587.7)	925.6 (890.2 – 960.7)	937.9 (920.5 – 966.8)		
B5					
Mean \pm SD.	-245.9 \pm 41	-106.1 ^a \pm 6.6	-104.2 ^a \pm 4.8	67.932*	<0.001*
Median (Min. – Max.)	228.7 (201.8 – 299.9)	106.2 (98.8 – 113.6)	103.1 (98.5 – 110.2)		
P5					
Mean \pm SD.	-858.1 \pm 28.5	-720.6 ^a \pm 28.3	-739.2 ^a \pm 20.4	49.396*	<0.001*
Median (Min. – Max.)	857.4 (821.3 – 890.4)	706.8 (699.5 – 769.1)	740.6 (710.1 – 766.4)		
Sum of mean microstrains around the abutments					
Mean \pm SD.	2856.6 \pm 82.9	2011.6 ^a \pm 28.6	2054 ^a \pm 33.5	463.01*	<0.001*
Median (Min. – Max.)	2845.9 (2752.2 – 2964.8)	2009.2 (1974.9 – 2054.5)	2041 (2030.8 – 2117.4)		
R6					
Mean \pm SD.	45.2 \pm 3.5	-27.5 ^a \pm 3.2	-29.9 ^a \pm 4	44.04*	<0.001*
Median (Min. – Max.)	44.6 (41.4 – 49.7)	26.8 (23.8 – 31.9)	29.4 (25.9 – 35.8)		
R7					
Mean \pm SD.	26.5 \pm 2.1	-153.5 ^a \pm 6.4	-157 ^a \pm 6.9	1077.7*	<0.001*
Median (Min. – Max.)	26.3 (23.9 – 29.3)	153.3 (145.3 – 160.8)	157.6 (147.6 – 165)		

SD: Standard deviation

F: F for ANOVA test, pairwise comparison between each two groups was done using Post Hoc Test (Tukey)

p: p value for comparing between the three studied groups.

a: Significant with group A

b: Significant with group B

*: Statistically significant at $p \leq 0.05$

Group A: The classical bilateral design.

Group B: Bilateral design with glass abutme

Group C: Unilateral design with glass abutment.

The negative sign in front of the mean denotes compression while absence of sign denotes tension following load application.

Table (2): Comparison between the recorded microstrain values ($\mu\text{m/m}$) for group A, B and C recorded at the examined sites under oblique load represented with range, mean and standard deviation.

Site of gauge	Group A (n = 6)	Group B (n = 6)	Group C (n = 6)	F	p
M4					
Mean \pm SD.	51.1 \pm 5.3	-231.4 ^a \pm 41.1	291.2 ^b \pm 10.1	154.31*	<0.001*
Median (Min. – Max.)	50.7 (45.7 – 58)	232.3 (183.1 – 274.2)	292.8 (277.6 – 301.8)		
B4					
Mean \pm SD.	-72.2 \pm 4.4	-42.5 ^a \pm 3.6	-52.1 ^b \pm 3.3	97.294*	<0.001*
Median (Min. – Max.)	71.9 (66.8 – 79.5)	43.2 (36.8 – 46)	51.8 (48.2 – 56.1)		
P4					
Mean \pm SD.	258.4 \pm 21	57 ^a \pm 5.7	399 ^b \pm 7.3	1007.5*	<0.001*
Median (Min. – Max.)	261.3 (225.4 – 279.7)	56.1 (50.2 – 64.5)	399.2 (387.4 – 408.1)		
D5					
Mean \pm SD.	-1254.2 \pm 40	-1093.3 ^a \pm 80.6	-1224.4 ^b \pm 25.1	15.110*	<0.001*
Median (Min. – Max.)	1253.3 (1200.8 – 1299.9)	1110.8 (997.3 – 1200.4)	1234.8 (1186.7 – 1250.2)		
B5					
Mean \pm SD.	-312.4 \pm 12.9	-36.3 ^a \pm 2.2	-37.6 ^a \pm 3.1	2535.7*	<0.001*
Median (Min. – Max.)	308.7 (299.9 – 330.9)	36.2 (33.1 – 39.6)	38.6 (32.8 – 40.8)		
P5					
Mean \pm SD.	950.4 \pm 33.7	857.2 ^a \pm 21	964.4 ^b \pm 8.9	36.85*	<0.001*
Median (Min. – Max.)	950.3 (899.7 – 990.9)	853.2 (830 – 890.6)	964.2 (950.5 – 975.4)		
Sum of mean microstrains around the abutments					
Mean \pm SD.	2898.8 \pm 85.8	2317.7 ^a \pm 81	2968.6 ^b \pm 35.1	151.85*	<0.001*
Median (Min. – Max.)	2909.9 (2773.5 – 3000.9)	2337.8 (2202.1 – 2394.1)	2978.9 (2921.5 – 3009.1)		
R6					
Mean \pm SD.	35.3 \pm 2.1	-20.8 ^a \pm 2.3	-28.7 ^b \pm 3.7	39.88*	<0.001*
Median (Min. – Max.)	35.5 (32.2 – 37.8)	21.2 (17.5 – 23.6)	28 (25 – 34)		
R7					
Mean \pm SD.	22.6 \pm 2.1	-111.8 ^a \pm 8.3	-96.6 ^b \pm 6.7	347.1*	<0.001*
Median (Min. – Max.)	22.5 (19.8 – 25.7)	114.1 (98.4 – 121.4)	97.7 (88.3 – 105.3)		

SD: Standard deviation

F: F for ANOVA test, pairwise comparison between each two groups was done using Post Hoc Test (Tukey)

p: p value for comparing between the three studied groups

a: Significant with group A

b: Significant with group B

*: Statistically significant at $p \leq 0.05$

Group A: The classical bilateral design.

Group B: Bilateral design with glass abutme

Group C: Unilateral design with glass abutment.

The negative sign in front of the mean denotes compression while absence of sign denotes tension following load application.

DISCUSSION

This study is the first to use the ZX-27 glass abutment system in RPD. The system was originally developed to be used in fixed partial

dentures to support the cantilevered pontic or pontics in long-span fixed bridges, by resting on the ridge, some of the masticatory load generated on the cantilevered pontic is transferred to the ridge, thereby reducing the damage to the abutment caused by vertical and oblique forces (9).

In RPDs the pontic teeth are already set to the denture base that transmits the masticatory loads to the ridge. The concept behind using the ZX-27 glass abutment system in this study relied on two properties in the glass abutment; the first was the adhesion properties of the borosilicate glass to create an anchorage point at the distal end of the DERPD. The vacuum and adhesion (10,11) may contribute to creating some sort of fixation of the denture base to the alveolar mucosa decreasing the movement of the denture base and hence the torque on the abutment teeth.

The second was the high modulus of elasticity (69,000 MPa) of the glass abutment (9), this high rigidity in comparison to the relatively lower rigidity of the denture base material (BioHPP) with a 4000 MPa modulus of elasticity (8) would help to absorb more loads directing them to the ridge away from the abutment teeth aiming to decrease the torque.

The structural engineering theory states that; in a structure made up of multiple structural elements where the surface distributing the forces to the elements is rigid, the elements will carry loads in proportion to their relative stiffness; the stiffer an element, the more load it will attract (18). This means that the glass abutment being more rigid than the BioHPP would help to absorb more loads directing them to the ridge away from the abutment teeth, aiming to decrease the torque on them.

The design in Group A and B "bilateral prosthesis" agreed with that mentioned in the academic dental literature. It followed the principle of cross-arch stabilization through a midpalatal strap major connector and a double Aker's clasp at the dentulous side. The indirect retention was provided by a mesial occlusal rest on the first premolar of the intact side. The width of the midpalatal strap major connector measured 10 mm for all the samples with bilateral design (group A and B) and the thickness of the strap and the framework was 1.4 mm (2,19).

The unilateral prosthesis design in group C was made without a major connector, but the buccal and palatal flanges extended to cover the buccal and palatal slopes of the residual ridge to provide some resistance to lateral movement in addition to compensation for lost tissues for maximum aesthetics (2,6,20).

Inspection of the microstrains recorded showed that the highest mean microstrains were always recorded at the distal aspect of the second premolar

abutment during both vertical and oblique loading in the three groups, which makes sense if we took into consideration the movement of the distal extension saddles caused by the RPD vertical displacement. An RPD held in place with a rigid telescopic connector acts as a class I stiff lever, that is to say, rigid pole with a fulcrum on one side (14,21,22).

Using the glass abutment, strains to the distal aspect have decreased in both groups that incorporated it (group B and C) than the classical design during both vertical and oblique loads. The difference was statistically significant in all situations except, during oblique loading in group C, the difference was insignificant.

Furthermore, the findings of our study revealed that, in all situations, the terminal abutment involved a greater risk than the mesial one, which was following Bergman et al. (23), who reported that at least two abutment teeth should be splinted when attachment prostheses are to be used for better stress pattern.

But, using the glass abutment, the microstrains records on the mesial and buccal aspects of the first premolar during vertical loading and the mesial aspect of it during oblique loading, have significantly increased, meaning better sharing of the first premolar in load-bearing, and better stress distribution.

Concerning the sum of microstrains acting on both of the abutments, group A demonstrated the significantly highest mean microstrains, followed by Group C, while Group B recorded the lowest mean microstrains. This could be attributed to the glass abutment action in load distribution between the abutment teeth and the ridge. Also, in spite of having higher mean microstrains the difference between Group C and B was insignificant, meaning that on using the glass abutment during vertical loading the cross-arch stabilization had an insignificant effect in decreasing the torque acting on the abutments and hence the microstrains conducted to them. This was in accordance with the findings of Wight in which no cross-arch stresses could be demonstrated and he concluded that the unilateral RPD produced no more stress than the bilateral one (4).

But, during oblique loading, the sum of microstrains acting on both of the abutments showed that; Group C demonstrated the highest mean microstrains followed by Group A while Group B recorded the lowest mean microstrains, this could be due to the tendency of the loads to be high on the abutment teeth in unilateral DERPDs to inhibit displacement of the denture base (5).

But despite having higher mean microstrains the difference between Group C and A was insignificant, which is coincident with Saito et al., who studied stress distribution and base

displacement in five different designs of Kennedy class II RPDs, they find out that, the displacement of the denture base tended to be less when the denture was designed with cross-arch stabilization. However, the difference was insignificant (6).

The higher microstrain values of the oblique loading compared to the vertical loading at the abutments in the three groups could be attributed to the fact that the non-axial forces tend to cause uneven stress distribution leading to areas of higher stresses and others of low stress (24).

Another observation was that the microstrains recorded at the ridge were extremely lower than that recorded at the abutment teeth, this is because the denture is 'rigidly' connected to the abutment teeth. According to the literature, the rigid telescopic attachment transmits the loads mainly to the abutment teeth, the more rigid the connection for the retainer the less would be the denture mobility and vice versa. Decreasing the RPD mobility is considered of great value regarding the maintenance of the residual ridge for DERPDs. Also, a more stable occlusion during occlusal functioning would contribute to the maintenance of the temporomandibular joint in the normal relationship and decrease the possibility of patient discomfort. Furthermore, the more the rigidity of the RPD retainer the less would be abutment mobility (25).

Strains recorded at the ridge in Group A during both vertical and oblique loading were tensile in nature. This could be explained by the flexion of the denture base under lever loading, as the BioHPP has relatively low flexure strength (150–330 MPa) (26). This flexion has been conducted to the supporting ridge as tensile stresses. In a previous study by Emera, et al that was concerned with evaluation and comparison of stresses applied to the implants retaining mandibular complete overdenture with telescopic attachments made of Zirconia and PEEK they explained the higher stress values recorded by all PEEK group by the less flexure strength of PEEK (150–330 MPa) in comparison to ZrO₂ (630–970 MPa) (27). Also, the tensile stresses to the ridge were coincident with a previous study by Bahgat, et al., (14) that was concerned with one treatment modality used for rehabilitation of mandibular Kennedy Class I cases, using two different materials, Co-Cr alloy and PEEK, and their effect on the strain induced in the supporting structures for these telescopic-retained (RPDs). The findings proved that PEEK telescopic retained RPDs resulted in statistically significant higher tensile strains in most of the channels when compared to Co-Cr RPD. They explained this result by the much higher Young's modulus of Co-Cr alloy (220–230 GPa) (28). Compared to that of the PEEK (3–4 GPa) (26) and concluded that Co-Cr alloy telescopic-retained RPD could still be considered a

better choice for rehabilitation of the Kennedy Class I partial edentulous situations compared to PEEK one, where Co-Cr generated less and better pattern of stresses to the denture-supporting structures (the residual alveolar ridges and abutments) (14).

Rigid major connectors resist deflection, deformation, and torquing forces that could be conducted to the supporting structures as destructive forces (29).

The inversion of the tensile stresses, that occurred on the ridge in group A during both loading conditions to more favorable compressive stresses in group B and C indicates a better pattern of stress distribution which intern decreased denture base bending under loads. The lack of these strains leads to a disuse mode (50–100 microstrain), in which remodeling tends to remove bone tissue while modeling tends to stay off. The physiologic strains might lie in the 100–2000 microstrain region. Supporting structures are more resistant to compression, tensile stresses from the eccentric contacts are likely to cause damage to the supporting structures (30).

Regarding the microstrain values recorded at the ridge during both of the loading conditions, in group A the microstrains to the ridge were concentrated at the site of the first molar during both loading conditions, as it was the site of load application, while in the groups with glass abutment, the microstrains were concentrated at the second molar site (the site of the glass abutment), this could be explained according to the structural engineering theory (18) by the ability of the glass abutment to attract the loads and directing them to the ridge. This also means better sharing of the ridge in load-bearing.

The mean microstrains recorded at the ridge were significantly higher during oblique loading at the site of the second molar (site of glass abutment) in group B than in group C. This could be due to the tendency of loading forces to move the denture base of the unilateral RPD around an axis perpendicular to the longitudinal axis of the ridge; hence movement occurs in a vertical direction towards the ridge. While in the case of the bilateral partial denture the rotation of the base occurred at an angle to the ridge, therefore the resultant vector of force was directed both vertical and lateral leading to more load conducted to the ridge. This was coincident with the findings of Aviv et al (31).

CONCLUSION

Within the limitation of this study and considering the test conditions, the following could be concluded:

The distal abutments always exhibit the highest microstrains, regardless of the loading conditions and the design of the prosthesis.

The use of glass abutment in association with the distal extension bases enhanced the load distribution pattern and decreased stresses conducted to the abutment teeth especially, at the distal aspect of the second premolar, by allowing the ridge and the first premolar abutment to share in load-bearing.

The stresses to the ridge have turned to be compressive in nature with the glass abutment use, which is more tolerable by the supporting ridge.

CONFLICT OF INTEREST

The authors declare that they have no conflict of interest.

FUNDING

The authors received no specific funding for this work.

REFERENCES

- Grasso JE, Miller EL. Removable partial prosthodontics. 2nd ed. B.C. Toronto, Philadelphia: Decker Inc; 2008. p137-51.
- Carr AB, Brown DT. McCracken's removable partial prosthodontics. 12th ed. St Louis: El Servier Mosby; 2011. p103-15p. 6, 21.
- Pruden II WH. A lower unilateral free-end partial denture. *J Prosthet Dent.* 1957;7:646-9.
- White JT. Visualization of stress and strain related to removable partial denture abutments. *J Prosthet Dent.* 1978;40:143-51.
- Aoda K, Shimamura I, Tahara Y, Sakurai K. Retainer design for unilateral extension base partial removable dental prosthesis by three-dimensional finite element analysis. *J Prosthodont Res.* 2010;54:84-91.
- Saito M, Miura Y, Notani K, Kawasaki T. Stress distribution of abutments and base displacement with precision attachment- and telescopic crown-retained removable partial dentures. *J Oral Rehabil.* 2003;30:482-7.
- Langer A. Telescope retainers and their clinical application. *J Prosthet Dent.* 1980;44:516-22.
- Zoidis P, Papathanasiou I, Polyzois G. The Use of a Modified Poly-Ether-Ether-Ketone (PEEK) as an Alternative Framework Material for Removable Dental Prostheses. A Clinical Report. *J Prosthodont.* 2016;25:580-4.
- Ramakrishaniah R, Al Kheraif AA, Elsharawy MA, Alsaleh AK, Ismail Mohamed KM, Rehman IU. A comparative finite elemental analysis of glass abutment supported and unsupported cantilever fixed partial denture. *Dent Mater.* 2015;31:514-21.
- Mihaela M. The use of zx27 bio-glass abutments in biterminal. *Romanian J Oral Rehabil.* 2013;5:45-50.
- The Attractive Glass Abutment System (ZX-27). 2017. Available at: <https://silo.tips/download/the-attractive-glass-abutment-system-zx-27-handout>.
- Williams RJ, Bibb R, Eggbeer D, Collis J. Use of CAD/CAM technology to fabricate a removable partial denture framework. *J Prosthet Dent.* 2006;96:96-9.
- Assunção WG, Barão VA, Tabata LF, Gomes EA, Delben JA, dos Santos PH. Biomechanics studies in dentistry: bioengineering applied in oral implantology. *J Craniofac Surg.* 2009;20:1173-7.
- Bahgat SF, El Homossany ME. Effect of material on stress transmission to the supporting structures in Kennedy Class I restored by Telescopic-retained Removable Partial Denture.(Strain Gauge Study). *Egypt Dent J.* 2018;64:559-73.
- Shahmiri R, Aarts JM, Bennani V, Das R, Swain MV. Strain Distribution in a Kennedy Class I Implant Assisted Removable Partial Denture under Various Loading Conditions. *Int J Dent.* 2013;2013:351279.
- Körber KH. Konuskronen. Das rationelle teleskopsystem einföhrung in klinik und technik. Heidelberg : Hüthig; 1988. p. 64-90.
- Horn TJ, Harrysson OL, Little JP, West II HA, Marcellin-Little DJ. Design and manufacturing of bone analog models for the mechanical evaluation of custom medical implants. In 21st Annual International Solid Freeform Fabrication Symposium-An Additive Manufacturing Conference, SFF 2010 2010. p. 864-875. University of Texas at Austin (freeform).
- Shinde SB, Raut NB. Effect of Change in Thicknesses and Height in Shear Wall on Deflection of Multistoried Buildings. *Technology.* 2016;7:587-91.
- Elsayed SR, Sherief DI, Selim MM, Alian GA. Strength of Different Major Connector Materials for Removable Partial Dentures. *Ain SDJ.* 2019;XXII:2-8.
- Radović K, Čairović A, Todorović A, Stančić I, Grbović A. Comparative analysis of unilateral removable partial denture and classical removable partial denture by using finite element method. *Srp Arh Celok Lek.* 2010;138:706-13.
- Heckmann SM, Winter W, Meyer M, Weber HP, Wichmann MG. Overdenture attachment selection and the loading of implant and denture-bearing area. Part 2: A methodical study using five types of attachment. *Clin Oral Implants Res.* 2001;12:640-7.
- Patnogić V, Todorović A, Šćepanović M, Radović K, Vesnić J, Grbović A. Free-end saddle length influence on stress level in unilateral complex partial denture abutment teeth and retention elements. *Vojnosanit Pregl.* 2013;70:1015-22.

23. Bergman B, Hugoson A, Olsson CO. Caries, periodontal and prosthetic findings in patients with removable partial dentures: a ten-year longitudinal study. *J Prosthet Dent.* 1982;48:506-14.
24. Barbier L, Vander Sloten J, Krzesinski G, Schepers E, Van der Perre G. Finite element analysis of non-axial versus axial loading of oral implants in the mandible of the dog. *J Oral Rehabil.* 1998;25:847-58.
25. Igarashi Y, Ogata A, Kuroiwa A, Wang CH. Stress distribution and abutment tooth mobility of distal-extension removable partial dentures with different retainers: an in vivo study. *J Oral Rehabil.* 1999;26:111-6.
26. Bayer S, Komor N, Kramer A, Albrecht D, Mericske-Stern R, Enkling N. Retention force of plastic clips on implant bars: a randomized controlled trial. *Clin Oral Implants Res.* 2012;23:1377-84.
27. Emera RM, Altonbary GY, Elbashir SA. Comparison between all zirconia, all PEEK, and zirconia-PEEK telescopic attachments for two implants retained mandibular complete overdentures: In vitro stress analysis study. *J Implant Dent* 2019;9:24.
28. Ogawa M, Tohma Y, Ohgushi H, Takakura Y, Tanaka Y. Early fixation of cobalt-chromium based alloy surgical implants to bone using a tissue-engineering approach. *Int J Mol Sci.* 2012;13:5528-41.
29. Stewart K, Rudd K, Kuebker W. *Clinical removable partial prosthodontics.* 2nd ed. St Louis, Tokyo: Ishiyaku Euro america Inc; 1992. p351-3.
30. Munari LS, Cornacchia TP, Moreira AN, Gonçalves JB, De Las Casas EB, Magalhães CS. Stress distribution in a premolar 3D model with anisotropic and isotropic enamel. *Med Biol Eng Comput.* 2015;53:751-8.
31. Aviv I, Ben-Ur Z, Cardash HS. An analysis of rotational movement of asymmetrical distal-extension removable partial dentures. *J Prosthet Dent.* 1989;61:211-4.